Article title: Safety margin evaluations for transtympanic laser stimulation of the cochlea from the outer ear in Mongolian gerbils (*Meriones unguiculatus*)

List of author names: Aya Okamoto[1], Miku Uenaka[1], Yuki Ito[1], Tomohiro Miyasaka[2], Koji Toda[3], Shizuko Hiryu[1], Kohta I. Kobayasi[1*], Yuta Tamai[1*]

Author affiliations:

[1]Neuroethology and Bioengineering, Graduate School of Life and Medical Sciences, Doshisha University, Kyotanabe, Kyoto, Japan

[2]Neuropathology, Graduate School of Life and Medical Sciences, Doshisha University, Kyotanabe, Kyoto, Japan

[3]Department of Psychology, Keio University, Tokyo, Japan

Corresponding author: Kohta I. Kobayasi and Yuta Tamai

(E-mail: kkobayas@mail.doshisha.ac.jp; ytamai@mail.doshisha.ac.jp)

Current address (Yuta Tamai): Neurobiology of Social Communication, Department of Otolaryngology-Head and Neck Surgery, Hearing Research Centre, University of Tübingen, Medical Center, Elfriede-Aulhorn-Strasse 5, 72076 Tübingen, Germany

Keywords

Auditory prosthesis, Infrared laser stimulation, Auditory perception, Head-fixed classical conditioning

Abstract

Infrared laser cochlear stimulation has been suggested as an alternative to traditional auditory prostheses. Previous research has mainly examined the short-term effects of laser stimulation, but to effectively use this technique, it is necessary to study whether prolonged laser exposure can safely and sustainably induce cochlear responses. This study assessed the effect of laser-induced cochlear damage using classically-conditioned Mongolian gerbils. The white noise was presented as a conditioned stimulus, and reward licking was recorded as a conditioned response. After training, the subject's cochlea was exposed to a continuous pulsed laser for 15 h. The licking rate drastically decreased after the exposure of 26.4 W/cm^2, while it did not change after 6.6 W/cm^2 or weaker. These findings showed, for the first time, that the safety margin of long-term, at least several hours, cochlear laser stimulation exists and will contribute to the safe and effective delimitation of laser parameters in future research.

38 **Introduction**

39 Hearing impairment is a prevalent sensory disorder worldwide. Approximately 466
40 million people, 5% of the world's population, suffer from hearing deficits, resulting in
41 severe communication difficulties and social isolation [1-3]. Hearing aids are among the
42 most widely used therapeutic options to compensate for these problems. These devices
43 improve speech comprehension and social interaction in hard-of-hearing individuals [4-6].
44 However, these patients require an intact middle ear to ensure sufficient and proper
45 hearing. Hard-of-hearing individuals with middle ear dysfunction must use an
46 implantable auditory prosthesis (e.g., bone-anchored hearing devices, middle ear implants,
47 or cochlear implants) that bypasses the function of the middle ear to stimulate the
48 peripheral auditory system. One of the most significant drawbacks preventing the
49 widespread use of these devices is surgical intervention, which increases the risk of
50 complications post-surgery [7-9].

51 Infrared laser stimulation has been discussed as a possible alternative to
52 conventional auditory devices [10]. The advantage of laser stimulation is that it can activate
53 spatially focused cell populations in a non-contact manner without the need to deliver any
54 exogenous agent into tissues, such as a viral vector [11]. Early research by Izzo *et al.* [12]
55 suggested that pulsed laser stimulation of the auditory nerves induced a cochlear response.

56 Several later studies that focused on the detailed relationship between the irradiation site
57 of the cochlea and laser-evoked neural response indicated that laser stimulation could
58 elicit spatially specific neural activities [13-16]. That is, precisely manipulating the laser
59 stimulation system can improve the spectral resolution of cochlear implants. Our previous
60 studies leveraged the benefit of the contactless feature of laser stimulation to reduce the
61 invasiveness of surgical implantation of the auditory prosthesis. They revealed that
62 transtympanic laser stimulation from the outer ear could evoke a cochlear response,
63 bypassing the middle ear function [17,18]. The auditory cortical activity elicited by
64 transtympanic laser stimulation depends on stimulus intensity [19]. These results imply that
65 a hearing prosthesis with infrared laser stimulation could be a noninvasive alternative to
66 the conventional implantable auditory prosthesis.

67 For the clinical application of transtympanic laser stimulation to auditory
68 prostheses, the safety margin of laser irradiation should be assessed. Because the laser-
69 evoked neural response is probably related to the thermal elevation of the tissue [20-22],
70 thermal build-up might be the main reason for laser-induced damage [23-25]. Therefore,
71 thermal damage to the peripheral auditory system can occur when a laser with high radiant
72 energy is continuously presented. Some studies have investigated laser irradiation trauma
73 in the cochlea [12,17,26,27]. Goyal *et al.* [28] compared the relationship between radiant energy

74 in continuous laser exposure and the reduction of the laser-evoked electrophysiological
75 response in the cochlea, reporting that the injury threshold for laser stimulation at 250 Hz
76 was between 25 and 30 μJ/pulse. However, no study has described the influence of laser-
77 induced thermal elevation on cochlear tissues or the effect of thermal physiological
78 damage on auditory perception.

79 A comprehensive evaluation of laser irradiation trauma elucidates the effects of
80 laser-induced damage on auditory perception. It provides a precise picture of the effect of
81 laser stimulation on the auditory peripheral system. It assessed laser-induced damage
82 characteristics of the peripheral auditory system by comparing electrophysiological,
83 histological, and behavioral alterations following continuous laser exposure. Here, we
84 performed (1) histological examination of spiral ganglions with hematoxylin and eosin
85 (HE) staining, (2) electrophysiological recording of the laser-evoked cochlear response
86 during laser irradiation, and (3) head-fixed classical conditioning with auditory stimulus
87 (see Fig. 1 for details).

88 This study performed a comprehensive safety evaluation of laser irradiation trauma
89 in Mongolian gerbils (*Meriones unguiculatus*). The Mongolian gerbil is a standard animal
90 model for investigating auditory physiology [e.g., 29,30,31]. Several studies have used gerbils
91 to investigate the mechanism of human speech perception because gerbils have a higher

92 sensitivity to the frequency range of human speech, including harmonics (250–3000 Hz),
93 than other rodents [32-35]. These studies suggest that the Mongolian gerbils is an excellent
94 animal model for studying the mechanism of human hearing. Furthermore, the anatomical
95 structure of the cochlea in gerbils is relatively large and shares several similarities with
96 humans compared to other rodents [36,37]. This anatomical similarity allows us to evaluate
97 the properties of laser-induced thermal distribution in the cochlea, which is essential data
98 for the clinical application of laser stimulation in hearing prostheses. Therefore, the safety
99 evaluation of transtympanic laser stimulation in Mongolian gerbils will help to establish
100 safe and effective laser stimulation parameters.

101

102 **Results**

103 *Continuous laser irradiation of 26.4 W/cm^2 or more increased the cochlear surface*
104 *temperature.*

105 Before the histological examination, the surface temperature of the cochlea was
106 recorded to investigate the thermal elevation following continuous laser irradiation (Fig.
107 2). The surface temperatures did not increase from 24 °C (i.e., room temperature) using
108 the 6.6 W/cm^2 laser irradiation or less; the laser 26.4 W/cm^2 or more increased the surface
109 temperatures immediately within 1 min into laser irradiation. The temperature rise

110 reached a plateau approximately 5 min after the laser onset (Fig. 2A). Average surface
111 temperature at 10 min after the laser irradiation onset was described in Fig. 2B and
112 showed that the increasing temperature induced by 26.4, 52.8, and 105.6 W/cm^2 lasers
113 were 31.6, 36.6, and 44.7 °C, respectively. The ANOVA revealed that the effect of radiant
114 energy was statistically significant ($F(5,17)=21.26$, $P<0.001$, one-way ANOVA). Fig. 2C
115 shows the lateral and medial surface temperatures induced by laser irradiation at 105.6
116 W/cm^2 on the lateral side of the cochlea. The average temperatures of the lateral and
117 medial sides resulted in approximately 41.2 and 32.5 °C, respectively, and the temperature
118 difference between the left and the right sides was statistically significant ($P<0.01$, paired
119 t-test). The medial side temperature was approximately in line with that of the lateral side
120 irradiated by the laser at 26.4–52.8 W/cm^2.
121
122 *Continuous laser irradiation mainly damaged the spiral ganglion neuron of the apical-*
123 *middle turn on the lateral side.*
124 Horizontal sections of the cochlea were subjected to HE staining to evaluate the
125 effect of laser exposure on the spiral ganglion neuron density (Fig. 3A). Lower spiral
126 ganglion neuron density was found in the cochlea continuously irradiated by the laser of
127 105.6 W/cm^2 than in less than 6.6 W/cm^2 (Fig. 3B). The middle turn of the cochlea

128 irradiated by the laser at 105.6 W/cm^2 is depicted in Fig. 3C. A comparison of the lateral
129 and medial sides showed a remarkable decrease in the cell density on the lateral side,
130 mainly irradiated by the transtympanic laser, compared to the medial side. On the lateral
131 side of the cochlea, the spiral ganglion density difference between the left and right ears
132 significantly decreased ($r=-0.87$, $P<0.05$, Pearson's correlation analysis) as radiant energy
133 intensified, whereas on the medial side, it did not ($r=-0.45$, $P=0.23$, Pearson's correlation
134 analysis) (Fig. 3D). The cell density decrement on the medial side after laser exposure of
135 105.6 W/cm^2 approximately coincides with that on the lateral side irradiated by the laser
136 with 26.4–52.8 W/cm^2. Fig. 3E shows the spiral ganglion neuron density difference on
137 the lateral side of the apical-middle and basal turn of the cochlea. The apical-middle turn
138 of the cell density in the left ear was significantly lower than that in the right ear ($P<0.05$,
139 one-sample t-test). In contrast, the basal turn of the cell density was less affected than the
140 apical-middle side ($P=0.19$, one-sample t-test) (Fig. 3E).
141
142 *The cochlear response with the laser of 26.4 W/cm^2 or more was reduced during the*
143 *continuous laser exposure.*
144 Fig. 4 shows the cochlear response during continuous laser exposure for 15 h. The
145 manifest damage in cochlear response was not observed by laser exposure up to 6.6

146 W/cm^2, while the cochlear response elicited by laser exposure of 105.6 W/cm^2 decreased

147 (Fig. 4A). The time course of the relative response amplitude showed that continuous

148 laser exposure at 105.6 W/cm^2 caused a drastic decrease in the laser-evoked response

149 amplitude within ca. 65 min (Fig. 4B). In comparison, laser irradiation of 6.6 W/cm^2 or

150 less did not. Fig. 4C shows the relationship between the laser irradiation time and

151 percentage of response amplitude. Laser irradiation over 26.4 W/cm^2 drastically increased

152 the average amplitude decrement, while laser stimulation with up to 26.4 W/cm^2 did not

153 (Fig. 4D).

154

155 *The continuous laser exposure within 6.6 W/cm^2 did not change the behavioral level,*

156 *while the 26.4 W/cm2 or more laser did.*

157 Fig. 5A shows the licking behavior evoked by white noise (80 dB SPL) before and

158 after 1.6, 6.6, and 105.6 W/cm^2 laser exposure. The laser exposure at 1.6 and 6.6 W/cm^2

159 did not cause an observable behavioral response change, while an apparent decrement of

160 the licking rate was observed after 105.6 W/cm^2 laser exposure. The behavioral changes

161 after laser exposure are depicted in Fig. 5B. Laser irradiation of the cochlea over 6.6

162 W/cm^2 drastically changed the behavioral level (Fig. 5B). It caused the delta behavioral

163 level (DBL) to reach out of the safety margin, which was calculated using three standard

164 deviations of DBL in the control condition (Fig. 5C).

165

166

167 **Discussion**

168 This study demonstrated that the laser stimulation with a higher average power
169 density triggered the thermal elevation of the cochlear surface (Fig. 2). Because the
170 conventional mechanism of the laser-evoked cochlear response is the optothermal effect,
171 which causes an excessive temperature increase in the cells [20-22], several studies indicated
172 that laser-induced thermal elevation and possible thermal-damage on the cochlea might
173 constitute a significant limitation in applying the laser to the auditory prosthesis [24,26-28,38].
174 Our study demonstrated that cochlear surface temperature significantly increased as
175 radiant energy increased (Fig. 2AB). The surface temperature continued to rise for
176 approximately 5 min after laser onset, and then the elevated temperature reached a plateau
177 (Fig. 2A). These results suggest that continuous laser irradiation (minute order) elevates
178 cochlear temperature compared with short-term irradiation. The continuous laser
179 irradiation at 105.6 W/cm^2 caused an average surface temperature up to 44.7 °C,
180 potentially causing thermal tissue damage [39]. These results demonstrate that continuous
181 laser stimulation bears the risk of thermal damage to the cochlear tissues when a laser
182 with high radiant energy is used.

183 A comparison of the thermal elevation of the cochlear surface with histological
184 damage of spiral ganglion neurons revealed that the thermal distribution of the cochlear

185 surface affected the laser irradiation trauma of the spiral ganglion neurons. Our previous
186 study showed that transtympanic lasers mainly irradiated the middle turn of the lateral
187 side of the cochlea [18]. This study implies that the highest peak of the thermal distribution
188 of the cochlear surface might be observed in the primary irradiated area, and the
189 temperature could decrease from the lateral to the medial side. It also showed that the
190 thermal elevation of the lateral side caused by laser irradiation of 105.6 W/cm^2 was
191 significantly higher than that on the medial side. The 105.6 W/cm^2 laser-induced
192 temperature rise of the medial side reached 32.5 °C, which agreed with the lateral side
193 temperature caused by the laser at 26.4–52.8 W/cm^2 (Fig. 2C). These results suggest that
194 approximately half of the radiant energy of laser irradiation reached the medial side of
195 the cochlea and agreed with the laser irradiation site in our previous study [18]. In addition,
196 a more significant decrease in cell density was observed on the lateral side of the apical-
197 middle turn than on the basal turn (Fig. 3E). These results coincide with the radiant energy
198 distribution (i.e., thermal distribution) of the cochlear surface and suggest that the spatial
199 injury profile of ganglion neurons depends on the thermal distribution of the cochlear
200 surface.

201 The electrophysiological cochlear response was recorded to evaluate the acute
202 damage threshold of continuous laser stimulation. This response is widely used as a

203 sensitive probe for physiological cochlear function [40-42]. Previous studies, including ours
204 [12,17,26], have assessed laser-irradiation trauma of the cochlea by recording the cochlear
205 response induced by continuous laser stimulation. These studies suggest that the laser
206 safely evokes cochlear responses without causing severe irradiation damage. However,
207 Goyal *et al.* [28] reported that continuous laser irradiation with higher radiant energy
208 induced thermal damage to the cochlear function. This indicates that the injury threshold
209 of laser exposure is between 25 and 30 μJ/pulse at 250 pulses/s (i.e., approximately 47.1
210 and 56.5 W/cm^2). Our results showed that the cochlea kept responding to laser stimulation
211 of 26.4 W/cm^2 or less, while the laser at 52.8 W/cm^2 or above remarkably decreased the
212 cochlear response (Fig. 4D). This result suggests that the electrophysiological damage
213 threshold of the laser stimulation is between 26.4 and 52.8 W/cm^2, and the injury
214 threshold is in line with the previous study by Goyal *et al.* [28].

215 Measuring the impact of thermal-induced physiological deterioration in the cochlea
216 on auditory perception is crucial. Behavioral assessment of hearing loss generally
217 provides compelling evidence of auditory perceptual consequences following
218 compromised auditory processing. Therefore, evaluating auditory perception following
219 thermal injury in the cochlea is an essential step toward the clinical application of laser
220 stimulation to auditory prostheses. This study showed that the auditory-evoked licking

221 behavior did not change after laser exposure of 6.6 W/cm^2 or weaker, but drastically
222 decreased after 26.4 W/cm^2 or above. These results suggest that the thermal injury
223 threshold for transtympanic laser stimulation is between 6.6 and 26.4 W/cm^2. Therefore,
224 transtympanic laser stimulation over 6.6 W/cm^2 could damage the subject's peripheral
225 auditory system and be out of the safety margin.

226 A comparison of the behavioral and electrophysiological results revealed that the
227 thermal damage threshold for the auditory-evoked behavior alteration was slightly lower
228 than that for the laser-evoked cochlear response. Here, the laser irradiates the tympanic
229 membrane, auditory ossicles, and cochlear tissues from the outer ear to induce the
230 cochlear response [18]; laser stimulation bears the risk of lesioning more peripheral auditory
231 function from the origin of the laser-evoked response. Our previous study revealed that
232 laser irradiation (λ=1871 nm) from the outer ear bypasses the tympanic membrane and
233 auditory ossicles because these tissues do not have higher absorbance to the infrared laser
234 [18]. However, some studies investigated the effect of the laser irradiation of the tympanic
235 membrane and auditory ossicles in *vivo* [43] and in *vitro* [44]. This indicates that the laser
236 irradiation of 27.9 W/cm^2 or above at 532 nm could cause thermal damage. Although
237 these results are not directly comparable to our data because of the difference in
238 wavelength-dependent absorbance in the tympanic membrane and auditory ossicles, as

239 some studies described [45-47], thermal damage to the tympanic membrane and auditory
240 ossicles might be one reason why continuous laser exposure affects the auditory-evoked
241 response more than the laser-evoked response.

242 In addition to the tympanic membrane and auditory ossicles, hair cells in the
243 cochlea can be damaged by laser irradiation. The physiological mechanism of the laser-
244 evoked cochlear response is still debated whether the response is hair-cell-mediated [11].
245 Hence, whether the laser-evoked response here characterized the state of cochlear
246 function is unclear, including that of hair cells. To reveal the physiological mechanism of
247 laser stimulation in the cochlea, some studies [48-50] compared laser-evoked auditory
248 responses in normal hearing and chemically compromised cochlea and reported that laser-
249 evoked auditory responses were only observed in the normal hearing cochlea. These
250 studies suggest that the cochlear response elicited by laser stimulation is mediated by hair
251 cells.

252 In contrast, Richter *et al.* [51] revealed that 30–40 dB chemical deafening of the
253 auditory threshold did not affect the threshold of the laser-evoked cochlear response. Tan
254 *et al.* [52] demonstrated that laser stimulation could elicit auditory neural activity in
255 congenitally deaf mice in which the cochlea could not transmit synapses between the
256 inner hair cells and spiral ganglion neurons.

In addition, when animals have an impaired hearing threshold, auditory masking does not affect laser-induced responses [53]. These results suggest that laser irradiation of the cochlea directly activates the auditory nerves, bypassing hair cells. If the laser activates the cochlear nerves without needing hair cell depolarization, the laser-evoked response does not characterize the state of the hair cells. Therefore, our results show that the auditory-evoked response might be more vulnerable to thermal injury than the laser-evoked response (Fig. 4 and 5). The effect of thermal damage to hair cells on laser-evoked cochlear responses must be considered in the future.

In summary, we assessed the laser-induced damage characteristics of the peripheral auditory system through histological, electrophysiological, and behavioral tests. Histological evaluation of the cochlea after continuous laser exposure revealed that the laser-induced thermal distribution of the cochlear surface coincided with the spatial injury profile of spiral ganglion neurons. The measurement of auditory-evoked behavioral and laser-evoked electrophysiological responses indicate that cochlear response during the laser exposure of 26.4 W/cm^2 or weaker did not decrease. In contrast, auditory-induced behavioral response drastically decreased after 26.4 W/cm^2 or higher. This discrepancy in the injury threshold suggests that laser stimulation bears the risk of lesioning more peripheral auditory functions from the origin of the laser-evoked response. Evaluating

perceptual consequences indicated that the thermal injury threshold for transtympanic laser stimulation in Mongolian gerbils is between 6.6 and 26.4 W/cm^2. Therefore, transtympanic laser under 6.6 W/cm^2 could be available without concern for acute injury. A comprehensive safety margin assessment is an essential step toward the practical application of transtympanic laser stimulation in auditory prostheses.

Limitations of the Study

One of the limitations of this research is that the safety of chronic transtympanic laser irradiation of the cochlea was not investigated. The present study showed that the transtympanic laser at a power of 6.6 W/cm^2 or weaker did not cause acute damage. However, hearing prostheses can be expected to be used over a long period of time, albeit intermittently rather than continuously. In order for transtympanic laser stimulation to be used in clinical applications, further studies on investigating the long-term safety of auditory perception needs to be conducted.

Another limitation is that safety on the human peripheral auditory organs has not been evaluated. Thermal damage from laser irradiation depends on the laser absorbance and tissue heat dissipation, which is related to the size and composition of the peripheral auditory system. Our previous study revealed that thicker tympanic membranes have

293 higher absorption; human tympanic membranes thicker those of gerbils might be at
294 greater risk for thermal damage [18]. As for the cochlea, the size of the cochlea is more
295 massive in humans than in gerbils [37]. Goyal et al. [28] discussed that the larger cochlea has
296 a higher rate at which heat is distributed and dissipated, suggesting that the energy
297 threshold for damage may be higher in humans than in small animals. Therefore, the
298 safety margin of the peripheral auditory system in humans might be different from our
299 current results. For practical application of transtympanic laser stimulation, a more
300 detailed evaluation of laser absorption and heat dissipation in the human peripheral
301 auditory system needs to be performed in the future.

302

303 **Materials and methods**

304 ***Animals***

305 All experimental procedures were performed according to the guidelines
306 established by the Ethics Review Committee of Doshisha University. The experimental
307 protocols were approved by the Animal Experimental Committee of Doshisha University.
308 A total of 33 experimentally naive Mongolian gerbils (fourteen females, nineteen males;
309 *Meriones unguiculatus*) aged 3–18 months were used here. All gerbils were bred and
310 reared in a laboratory. Each animal was housed with 2–5 gerbils in a 20 (W) × 40 (L) ×

311 17 cm (H) cage, with free access to food and water. The animal room had a 12-h light-
312 dark schedule, a temperature of 22–23 °C, and relative humidity of approximately 50%.
313 All subjects were randomly assigned to each experimental group.

314 ***Animal surgery***

315 Mongolian gerbils were deeply anesthetized with ketamine (47 mg/kg i.m.) and
316 xylazine (9.3 mg/kg i.m.). Maintenance doses of ketamine (17.5 mg/kg) and xylazine (7.0
317 mg/kg) were injected every 30–50 min or if the animals showed signs of increasing
318 arousal (e.g., voluntary whisker movement). The body temperature of the gerbils was
319 maintained using heating pads placed beneath the animals. The left side of the bulla was
320 exposed by incision of the muscle and skin from the shoulder to the jaw, and a hole
321 (diameter: 1 mm) was made on the bulla. A silver electrode (Nilaco, Tokyo, Japan;
322 diameter: 0.13 mm; impedance < 20 kΩ) was inserted into the hole and hooked onto the
323 bony rim of the round window to record cochlear responses. The electrode was stabilized
324 with a bulla using acrylic glue and dental cement (Provinice; Shofu, Kyoto, Japan). The
325 left pinna was removed to provide a clear view of the tympanic membrane. A liquid of
326 acrylic glue and dental cement (Provinice; Shofu, Kyoto, Japan) was mounted into the
327 right ear for approximately 50 dB SPL attenuation of the sound pressure reaching the right
328 ear.

329 The parietal and temporal sides of the fur and the skin of the subject's head were
330 shaved. The temporal muscle was removed after applying a local anesthetic (xylocaine
331 gel; Aspen Japan, Tokyo, Japan). The skull was carefully cleaned with 0.3% sodium

332 hypochlorite solution and saline. A small hole was made in the dorsal skull 2 mm anterior
333 to the bregma and 1 mm lateral to the midline, and a reference electrode was inserted into
334 the hole. A V-shaped metal plate (F-911; Hilogik, Osaka, Japan) was attached to the skull
335 using acrylic dental resin (Super bond C&B; Sun Medical, Shiga, Japan) and dental
336 cement (Provinice; Shofu, Kyoto, Japan), allowing the subjects to be head-fixed during
337 the experiment. All subjects were singly housed during recovery for at least two days
338 before training began.

339 ***Auditory stimuli***

340 White noise (700–44,800 Hz) was used as an auditory stimulus, with a duration of
341 500 ms. The auditory stimulus was presented via a doom tweeter (FT28D; Fostex, Tokyo,
342 Japan) from 15 cm above the subject's head. The stimulus was generated using a digital-
343 to-analog converter (Octa-Capture; Roland, Shizuoka, Japan) with a sampling rate of 192
344 kHz. The signal was intensified using an amplifier (A-10; Pioneer, Tokyo, Japan). The
345 sound pressure level was calibrated to 20, 35, 50, 65, 80, and 95 dB SPL using a
346 microphone (Type 7016; Aco, Tokyo, Japan).

347 ***Apparatus and procedure in the behavioral experiment***

348 Behavioral experiments were conducted in a soundproof box 60 (W) × 60 (L) × 60
349 cm (H). Licking recordings in head-fixed animals were performed as previously described

350 [54-57]. Each subject was positioned on a covered elevated platform (custom-designed and
351 3D printed). A drinking spout was placed 1 mm in front of the mouth of the animal, and
352 the clamp and drinking spout positions were adjusted to detect licking behavior easily. A
353 touch sensor (DCTS-10; Sankei Kizai, Tokyo, Japan), connected between the drinking
354 spout and the metal sheet of the stage, recorded the timing of licks at 2000 samples/s. The
355 recorded licking timing was stored on a computer via Arduino Uno (Arduino, Ivrea, Italy)
356 controlled by Python 3.7 on Spyder 501. All behaviors were recorded using a video
357 camera (HD-5000; Microsoft, Washington, USA).

358 After at least 2 days of recovery from surgery, the gerbils were water-restricted
359 in their home cage. The training session typically comprised 400 trials daily. Head-fixed
360 participants were allowed to voluntarily lick the spout at all times. A 3.2 μl drop of water
361 (unconditioned stimulus: US) was delivered through the tube every 7–13 s after
362 presenting an 85 dB SPL of white noise (conditioned stimulus: CS) controlled by
363 MATLAB (MathWorks, Massachusetts, USA) and a microcontroller (Arduino Uno;
364 Arduino, Ivrea, Italy) with a custom-made relay circuit.

365 After animals showed high licking rates following the auditory cue, catch trials
366 were conducted to evaluate the subject's perception. The test session comprised rewarded
367 and non-rewarded trials (i.e., catch trials). Catch trials were included to assess the subjects'

368 perceptions without reward feedback. White noise of 20, 35, 50, 65, 80, or 95 dB SPL
369 was presented in the catch trials. During a test session, 280 rewarded trials and 120 catch
370 trials were conducted in a pseudo-random order. In the catch trials, each sound intensity
371 was tested 20 times. The test session was performed pre- and post-laser exposure.

372 ***Recording and analysis of the behavioral data***

373 An averaged histogram of licking behavior was used to evaluate the time course of
374 behavioral responses. The histograms were calculated in a 100 ms bin size and
375 smoothened using a 300-ms moving average window. Peak licking rates, durations, peak
376 latencies, and response latencies were extracted from the time course of licking behavior
377 to assess the behavioral response. Peak licking rates and peak latencies were defined as
378 the licking rate and time when the licking rate reached the maximum value within 4 s
379 after stimulus onset, respectively. The baseline licking rate was defined as the pre-
380 stimulus licking rate obtained for 1 s, and duration was quantified as the temporal length
381 of licking behavior >50% of the licking rate from the mean baseline licking rate to the
382 peak licking rate. Response latency was determined by measuring the time between
383 stimulus onset and the behavioral response reaching the mean plus three standard
384 deviations of the baseline licking rate. The delta licking rate was defined as the difference
385 between the mean baseline licking rate and the post-stimulus licking rate to evaluate the

386 response amplitude. The analysis range of post-stimulus licking behavior was 0.2–1.2 s
387 because the behavioral response was mostly observed 0.2 s after stimulus onset (see
388 Supplemental Fig. 1 for details). The behavioral level was calculated by standardizing the
389 highest delta licking behavior in the pre-exposure test. The delta behavioral level (DBL)
390 between the pre- and post-exposure test was defined as the summation of the difference
391 in the behavioral level for all sound pressure levels to evaluate the effect of continuous
392 laser exposure on auditory perception.

393 ***Laser exposure***

394 A repetitive pulsed infrared laser was used for laser exposure. The individual pulse
395 of the laser had a 100 μs rectangular shape in intensity. It was generated using a diode
396 laser stimulation system (BWF-OEM-1850; B&W TEK, Delaware, USA) with a
397 wavelength (λ=1871) comparable to those previously reported [12,38,50]. The voltage
398 commands for the laser stimuli were generated using a function generator (WF1974; NF,
399 Kanagawa, Japan). The repetition frequency of the pulsed laser was changed to 125, 250,
400 500, 2000, 4000, and 8000 Hz to adjust the amount of radiant energy reaching the cochlea
401 to 1.6, 3.3, 6,6, 26.4, 52.8, and 105.6 W/cm^2, respectively. The radiant energy and beam
402 width at the cochlea (i.e., 2.2 mm from the fiber tip) were measured using a digital power
403 meter (PM100D; Thorlabs, Tokyo, Japan) with a thermal power sensor (S302C; Thorlabs,
404 Tokyo, Japan) and an InGaAs biased detector (DET10D/M; Thorlabs, Tokyo, Japan),
405 respectively. Our previous study measured the laser-beam profile [18].

406 An optic fiber (diameter: 100 μm; NA, 0.22) was inserted mediolaterally into the

407 left outer ear canal with the tip angled rostrally by 10° and dorsally by 5° using a
408 micromanipulator (MM-3; Narishige, Tokyo, Japan) in awake head-fixated subjects. The
409 optic fiber tip was set at c.a. 0.7 mm in front of the tympanic membrane to ensure that the
410 cochlea was irradiated transtympanically from the outer ear as described in our previous
411 reports [17-19].

412 Each subject's cochlea was continuously stimulated by laser irradiation from the
413 outer ear for 15 h. Continuous laser exposure was performed on the same covered elevated
414 platform in the soundproof box as in the behavioral experiment. The temperature in the
415 soundproof box was adjusted to approximately 26 ℃, and a small pee pad was placed
416 beneath the subject to prevent the subject's temperature from decreasing. After laser
417 exposure and behavioral experiments, the subjects were overdosed with an intraperitoneal
418 injection of pentobarbital (200 mg/kg). Laser-induced cochlear response was
419 continuously recorded throughout the study period. The cochleae were histologically
420 investigated to clarify the thermal damage caused by laser irradiation.

421 ***Recording and analysis of the cochlear response during laser exposure***

422 After the pre-exposure test, cochlear response was recorded in awake subjects
423 during continuous laser exposure. The cochlear response was amplified 1000 times using
424 a bio-amplifier (MEG-1200; Nihon Kohden, Tokyo, Japan) and stored on a computer via
425 an analog-to-digital converter (Octa-capture; Roland, Shizuoka, Japan) at a sampling rate
426 of 96,000 Hz.

427 The recorded signal was processed using a band-pass filter (100–10,000 Hz) and
428 separated at 10 ms intervals. The cochlear signal was averaged 1000 times every 10 s for
429 15 h, and the response amplitude of the averaged cochlear signal was evaluated using the

430 amplitude spectrum distribution. To obtain high-frequency resolution, 32,768 points of
431 zero paddings were performed on the head and end of the averaged signal. The amplitude
432 spectrum was extracted using fast Fourier transforms (FFT, 16,384 points with a Hanning
433 window); therefore, the frequency resolution was 5.9 Hz. The peak of the amplitude
434 spectrum at the stimulus repetition frequency was extracted as the response amplitude.
435 The mean response amplitude was calculated at 5 min intervals standardized by the first
436 5 min mean amplitude.

437 ***Preparation of histological evaluation***

438 Following the post-exposure test session, the laser-irradiated subjects were
439 euthanized by an overdose of pentobarbital (200 mg/kg i.p.). After postmortem perfusion
440 with phosphate buffered saline (PBS) and 4% paraformaldehyde in PBS, the animals were
441 decapitated and fixed in the same fixative for two days in a refrigerator at 4 ℃.
442 Subsequently, the tissues were stored in cooled PBS containing 0.02% sodium azide.

443 The paraformaldehyde-fixed tissues were decalcified by immersing in a mixture
444 solution of formic acid (0.28 g/ml), citric acid (0.1 g/ml), and sodium hydroxide (0.02
445 g/ml) for 7–10 days. The decalcifying solution was exchanged every 2–3 days. After the
446 decalcification, the samples were preserved in PBS with 0.02% sodium azide.

447 Decalcified head tissues were dehydrated using a gradually ascending
448 concentration of ethanol (70–100%) for 2 days followed by immersion in 100% xylene

449 and embedding into a paraffin block. Horizontally, paraffin-embedded sections with the
450 thickness of 6 μm was processed using a microtome (HM 430; Thermo, Tokyo, Japan).
451 Cochlear sections between 7 and 8 mm ventral to the sagittal midline from each
452 subject were examined. Sections were deparaffinized by immersion in 100% xylene.
453 After the deparaffinization, sections were hydrated with 100% ethanol and distilled water.
454 Sections were stained with Mayer's hematoxylin solution and rinsed with distilled water.
455 After differentiation with 70% ethanol containing 0.1% HCL, the sections were stained
456 with Putt's eosin solution. HE-stained sections were re-immersed in 100% ethanol and
457 cleared in xylene. All stained sections were mounted in mounting medium (HSR solution;
458 Sysmex, Hyogo, Japan). Specimens were photographed using a digital camera (BX53;
459 Olympus, Tokyo, Japan) under a light microscope (EX-F1; Casio, Tokyo, Japan).
460 Histological analysis was performed using ImageJ software [58,59]. The main part of the
461 analyzed spiral ganglions might be afferent Type-I neurons because they are 95 % of the
462 total population of the spiral ganglion.
463 ***Behavioral data analysis for a safety margin evaluation***
464 Each subject was placed on a covered elevated platform for 15 h in a temperature-
465 controlled soundproof box, similar to the laser exposure experiment without presenting
466 laser irradiation. We compared the performance of the classical conditioning task before

467 and after placement on the covered elevated platform. The mean and standard deviation
468 of the control condition were measured to determine the safety margin of continuous laser
469 irradiation. The safety margin was defined as the mean ± three standard deviations of
470 the DBL in the control condition (n=9).

471 ***Correlation between physiological damage in the cochlea and behavioral alternation***

472 To determine whether these histological and functional deficits in the cochlea were
473 associated with behavioral alterations, we correlated the change in spiral ganglion neuron
474 density and amplitude of the cochlear response with the behavioral response. Further
475 details are provided in Supplemental Fig. 2.

476 ***Recording thermal elevation of the cochlear surface***

477 Eleven gerbils were euthanized (pentobarbital; 200 mg/kg) and decapitated for
478 cochlear surface thermal measurements. Both sides of the cochlea were extracted from
479 the skulls under a stereomicroscope. The cochlea was placed in a Petri dish and stabilized
480 with dental wax. The laser fiber tip was directed vertically to the surface of the cochlea
481 and was set to 2.2 mm from the cochlear surface. Continuous laser irradiation with 1.6,
482 3.3, 6.6, 26.4, 52.8, and 105.6 W/cm^2 was performed for 1 h, and the surface temperature
483 elevations were measured using a thermal camera (FLIR C3-X; Teledyne FLIR LLC,
484 Oregon, USA), which was positioned at 21 cm from the cochlear surface with vertically

485 45° angle.

486 To acquire the thermal elevation on the lateral and medial sides of the cochlear
487 surface, a thermocouple (MSM-3905; Biomedica, Osaka, Japan) was used. The tip of the
488 thermocouple sensor was in contact with the second turn of the cochlear surface on one
489 side for 1 h. After recording the temperature on one side, the specimen was left for at least
490 15 min to cool down to room temperature (~24 °C), and then the temperature on another
491 side was measured.

492 ***Flow of the behavioral, electrophysiological, and histological procedure***

493 Surgery, behavior training, pre-exposure test, laser exposure for 15 h, post-exposure
494 test, and histological evaluation were performed in this order. The recovery period was
495 performed after surgery before and after laser exposure. Further details are provided in
496 Fig. 1.

497

498 **Acknowledgement**

499 The authors would like to thank Hiroshi Riquimaroux for his support during the
500 early stages of this work. We also thank Kazuki Tanaka, Mizuki Katayama, and Keito
501 Hosokawa for technical support and Editage (www.editage.com) for English language
502 editing. This research was financially supported by the Sasakawa Scientific Research

Grant No. 2022–6027 (A.O.), the Japan Society for the Promotion of Science (JSPS) KAKENHI Grants Nos. 22H02946 (T.M.), 21H03469 (K.I.K.), 21K21322 (Y.T.), the JSPS Overseas Research Fellowship (Y.T.), and Keio Academic Development Fund (K.T.).

Author contribution

Conceptualization: A.O., KI.K., and Y.T.; Data curation: A.O. and M.U.; Formal analysis: A.O. and Y.T.; Funding acquisition: A.O., T.M., K.T., KI.K., and Y.T.; Investigation: A.O. and Y.T.; Methodology: Y.I., T.M., and K.T.; Project administration: KI.K. and Y.T.; Software: A.O. and Y.T.; Supervision: S.H.; Validation: A.O.; Visualization: A.O. and Y.T.; Writing-Original Draft: A.O. and Y.T.; Writing-Review&Editing: A.O., M.U., Y.I., T.M., K.T., S.H., KI.K., and Y.T.

Conflict of interests

The authors have no conflicts of interest to declare.

Data availability statement

All data needed to evaluate the conclusions are shown in the paper and supplemental figures. Additional data related to this paper are available from the corresponding author upon reasonable request.

References

1. World Health Organization (2018). Addressing the rising prevalence of hearing loss. Available at: https://apps.who.int/iris/handle/10665/260336 [Accessed 7 September 2022].
2. World Health Organization (2019). New WHO-ITU standard aims to prevent hearing loss among 1.1 billion young people. Available at: https://www.who.int/news/item/12-02-2019-new-who-itu-standard-aims-to-prevent-hearing-loss-among-1.1-billion-young-people [Accessed 7 September 2022].
3. World Health Organization (2021). Deafness and hearing loss. Available at: https://www.who.int/news-room/fact-sheets/detail/deafness-and-hearing-loss [Accessed 7 September 2022].
4. Mulrow, C.D., Aguilar, C., Endicott, J.E., Tuley, M.R., Velez, R., Charlip, W.S., Rhodes, M.C., Hill, J.A., and DeNino, L.A. (1990). Quality-of-life changes and hearing impairment. A randomized trial. Ann. Intern. Med. *113*, 188-194. 10.7326/0003-4819-113-3-188.
5. Mulrow, C.D., Tuley, M.R., and Aguilar, C. (1992). Sustained benefits of hearing aids. J. Speech Hear. Res. *35*, 1402-1405. 10.1044/jshr.3506.1402.
6. Arlinger, S. (2003). Negative consequences of uncorrected hearing loss-a review. Int. J. Audiol. *42 Suppl 2*, 2s17-20.
7. Håkansson, B., Eeg-Olofsson, M., Reinfeldt, S., Stenfelt, S., and Granström, G. (2008). Percutaneous versus transcutaneous bone conduction implant system: A feasibility study on a cadaver head. Otol. Neurotol. *29*, 1132-1139. 10.1097/MAO.0b013e31816fdc90.
8. Yeung, J., Griffin, A., Newton, S., Kenna, M., and Licameli, G.R. (2018). Revision cochlear implant surgery in children: Surgical and audiological outcomes. Laryngoscope *128*, 2619-2624. 10.1002/lary.27198.
9. Ahmed, J., Saqulain, G., Khan, M.I.J., and Kausar, M. (2021). Complications of cochlear implant surgery: A public implant centre experience. Pak. J. Med. Sci. *37*, 1519-1523. 10.12669/pjms.37.5.3960.
10. Littlefield, P.D., and Richter, C.P. (2021). Near-infrared stimulation of the auditory nerve: A decade of progress toward an optical cochlear implant. Laryngoscope Investig. Otolaryngol. *6*, 310-319. 10.1002/lio2.541.
11. Fekete, Z., Horváth, Á.C., and Zátonyi, A. (2020). Infrared neuromodulation: A neuroengineering perspective. J. Neural Eng. *17*, 051003. 10.1088/1741-

2552/abb3b2.

12. Izzo, A.D., Richter, C.P., Jansen, E.D., and Walsh Jr., J.T. (2006). Laser stimulation of the auditory nerve. Lasers Surg. Med. *38*, 745-753. 10.1002/lsm.20358.

13. Izzo, A.D., Suh, E., Pathria, J., Walsh, J.T., Whitlon, D.S., and Richter, C.P. (2007). Selectivity of neural stimulation in the auditory system: A comparison of optic and electric stimuli. J. Biomed. Opt. *12*, 021008. 10.1117/1.2714296.

14. Matic, A.I., Walsh, J.T., Jr., and Richter, C.P. (2011). Spatial extent of cochlear infrared neural stimulation determined by tone-on-light masking. J. Biomed. Opt. *16*, 118002. 10.1117/1.3655590.

15. Moreno, L.E., Rajguru, S.M., Matic, A.I., Yerram, N., Robinson, A.M., Hwang, M., Stock, S., and Richter, C.P. (2011). Infrared neural stimulation: Beam path in the guinea pig cochlea. Hear. Res. *282*, 289-302. 10.1016/j.heares.2011.06.006.

16. Richter, C.P., Rajguru, S.M., Matic, A.I., Moreno, E.L., Fishman, A.J., Robinson, A.M., Suh, E., and Walsh, J.T. (2011). Spread of cochlear excitation during stimulation with pulsed infrared radiation: Inferior colliculus measurements. J. Neural Eng. *8*, 056006. 10.1088/1741-2560/8/5/056006.

17. Tamai, Y., Horinouchi, K., Hiryu, S., and Kobayasi, K.I. (2019). Infrared laser stimulation of cochlear nerve through a tympanic membrane. Conf. Proc. IEEE Life Sci. Tech. 2019 *1*, 54-57. 10.1109/LifeTech.2019.8884023.

18. Uenaka, M., Nagamura, H., Hiryu, S., Kobayasi, K.I., and Tamai, Y. (2022). Feasibility evaluation of transtympanic laser stimulation of the cochlea from the outer ear. J. Acoust. Soc. Am. *152*, 1850-1855. 10.1121/10.0014241.

19. Tamai, Y., Ito, Y., Furuyama, T., Horinouchi, K., Murashima, N., Michimoto, I., Hishida, R., Shibuki, K., Hiryu, S., and Kobayasi, K.I. (2020). Auditory cortical activity elicited by infrared laser irradiation from the outer ear in Mongolian gerbils. PloS one *15*, e0240227. 10.1371/journal.pone.0240227.

20. Wells, J., Kao, C., Konrad, P., Milner, T., Kim, J., Mahadevan-Jansen, A., and Jansen, E.D. (2007). Biophysical mechanisms of transient optical stimulation of peripheral nerve. Biophys. J *93*, 2567-2580. 10.1529/biophysj.107.104786.

21. Shapiro, M.G., Homma, K., Villarreal, S., Richter, C.P., and Bezanilla, F. (2012). Infrared light excites cells by changing their electrical capacitance. Nat. Commun. *3*, 736. 10.1038/ncomms1742.

22. Albert, E.S., Bec, J.M., Desmadryl, G., Chekroud, K., Travo, C., Gaboyard, S., Bardin, F., Marc, I., Dumas, M., Lenaers, G., et al. (2012). TRPV4 channels

mediate the infrared laser-evoked response in sensory neurons. J. Neurophysiol. *107*, 3227-3234. 10.1152/jn.00424.2011.

23. Chernov, M.M., Chen, G., and Roe, A.W. (2014). Histological assessment of thermal damage in the brain following infrared neural stimulation. Brain. Stimul. *7*, 476-482. 10.1016/j.brs.2014.01.006.

24. Thompson, A.C., Wade, S.A., Pawsey, N.C., and Stoddart, P.R. (2013). Infrared neural stimulation: Influence of stimulation site spacing and repetition rates on heating. IEEE Trans. Biomed. Eng. *60*, 3534-3541. 10.1109/TBME.2013.2272796.

25. Brown, W.G.A., Needham, K., Begeng, J.M., Thompson, A.C., Nayagam, B.A., Kameneva, T., and Stoddart, P.R. (2020). Thermal damage threshold of neurons during infrared stimulation. Biomed. Opt. Express *11*, 2224-2234. 10.1364/boe.383165.

26. Rajguru, S.M., Matic, A.I., Robinson, A.M., Fishman, A.J., Moreno, L.E., Bradley, A., Vujanovic, I., Breen, J., Wells, J.D., Bendett, M., and Richter, C.P. (2010). Optical cochlear implants: evaluation of surgical approach and laser parameters in cats. Hear. Res. *269*, 102-111. 10.1016/j.heares.2010.06.021.

27. Matic, A.I., Robinson, A.M., Young, H.K., Badofsky, B., Rajguru, S.M., Stock, S., and Richter, C.P. (2013). Behavioral and electrophysiological responses evoked by chronic infrared neural stimulation of the cochlea. PloS one *8*, e58189. 10.1371/journal.pone.0058189.

28. Goyal, V., Rajguru, S., Matic, A.I., Stock, S.R., and Richter, C.P. (2012). Acute damage threshold for infrared neural stimulation of the cochlea: functional and histological evaluation. Anat. Rec. (Hoboken) *295*, 1987-1999. 10.1002/ar.22583.

29. Ohl, F.W., and Scheich, H. (2005). Learning-induced plasticity in animal and human auditory cortex. Curr. Opin. Neurobiol. *15*, 470-477. 10.1016/j.conb.2005.07.002.

30. Budinger, E., and Scheich, H. (2009). Anatomical connections suitable for the direct processing of neuronal information of different modalities via the rodent primary auditory cortex. Hear. Res. *258*, 16-27. 10.1016/j.heares.2009.04.021.

31. Ryan, A. (1976). Hearing sensitivity of the mongolian gerbil, Meriones unguiculatis. J. Acoust. Soc. Am. *59*, 1222-1226. 10.1121/1.380961.

32. Ohl, F.W., and Scheich, H. (1997). Orderly cortical representation of vowels based on formant interaction. Proc. Natl. Acad. Sci. U S A *94*, 9440-9444. 10.1073/pnas.94.17.9440.

33. Sinnott, J.M., Street, S.L., Mosteller, K.W., and Williamson, T.L. (1997). Behavioral measures of vowel sensitivity in Mongolian gerbils (Meriones unguiculatus): effects of age and genetic origin. Hear. Res. *112*, 235-246. 10.1016/s0378-5955(97)00125-1.

34. Schebesch, G., Lingner, A., Firzlaff, U., Wiegrebe, L., and Grothe, B. (2010). Perception and neural representation of size-variant human vowels in the Mongolian gerbil (Meriones unguiculatus). Hear. Res. *261*, 1-8. 10.1016/j.heares.2009.12.016.

35. Jüchter, C., Beutelmann, R., and Klump, G.M. (2022). Speech sound discrimination by Mongolian gerbils. Hear. Res. *418*, 108472. 10.1016/j.heares.2022.108472.

36. Abbas, L., and Rivolta, M.N. (2015). Aminoglycoside ototoxicity and hair cell ablation in the adult gerbil: a simple model to study hair cell loss and regeneration. Hear. Res. *325*, 12-26. 10.1016/j.heares.2015.03.002.

37. Keppeler, D., Kampshoff, C.A., Thirumalai, A., Duque-Afonso, C.J., Schaeper, J.J., Quilitz, T., Töpperwien, M., Vogl, C., Hessler, R., Meyer, A., et al. (2021). Multiscale photonic imaging of the native and implanted cochlea. Proc. Natl. Acad. Sci. U S A *118*. 10.1073/pnas.2014472118.

38. Izzo, A.D., Walsh Jr., J.T., Jansen, E.D., Bendett, M., Webb, J., Ralph, H., and Richter, C.P. (2007). Optical parameter variability in laser nerve stimulation: A study of pulse duration, repetition rate, and wavelength. IEEE Trans. Biomed. Eng. *54*, 1108-1114. 10.1109/TBME.2007.892925.

39. Dewey, W.C. (1994). Arrhenius relationships from the molecule and cell to the clinic. Int. J. Hyperthermia *10*, 457-483. 10.3109/02656739409009351.

40. van Eijl, R.H., Buitenhuis, P.J., Stegeman, I., Klis, S.F., and Grolman, W. (2017). Systematic review of compound action potentials as predictors for cochlear implant performance. Laryngoscope *127*, 476-487. 10.1002/lary.26154.

41. Prado-Guitierrez, P., Fewster, L.M., Heasman, J.M., McKay, C.M., and Shepherd, R.K. (2006). Effect of interphase gap and pulse duration on electrically evoked potentials is correlated with auditory nerve survival. Hear. Res. *215*, 47-55. 10.1016/j.heares.2006.03.006.

42. Ramekers, D., Versnel, H., Strahl, S.B., Klis, S.F., and Grolman, W. (2015). Recovery characteristics of the electrically stimulated auditory nerve in deafened guinea pigs: Relation to neuronal status. Hear. Res. *321*, 12-24. 10.1016/j.heares.2015.01.001.

43. Sorg, K., Stahn, P., Pillong, L., Hinsberger, M.P., Heimann, L., Foth, H.J., Schick, B., and Wenzel, G.I. (2019). First biocompatibility margins for optical stimulation at the eardrum via 532-nm laser pulses in a mouse model. J. Biomed. Opt. *24*, 085003. 10.1117/1.Jbo.24.8.085003.
44. Pillong, L., Stahn, P., Hinsberger, M., Sorg, K., Schick, B., and Wenzel, G.I. (2020). Cytotoxicity studies of an optoacoustic stimulation strategy for the development of laser-based hearing aids. J. Biomed. Opt. *25*, 068002. 10.1117/1.Jbo.25.6.068002.
45. Goblet, M., Matin, F., Lenarz, T., and Paasche, G. (2021). Optical absorbance of the tympanic membrane in rat and human samples. PloS one *16*, e0254902. 10.1371/journal.pone.0254902.
46. Carr, J.A., Valdez, T.A., Bruns, O.T., and Bawendi, M.G. (2016). Using the shortwave infrared to image middle ear pathologies. Proc. Natl. Acad. Sci. U S A *113*, 9989-9994. 10.1073/pnas.1610529113.
47. Heimann, L., Carlein, C., Sorg, K., Diller, R., Langenbucher, A., Schick, B., and Wenzel, G.I. (2021). Wavelength-specific optoacoustic-induced vibrations of the guinea pig tympanic membrane. J. Biomed. Opt. *26*, 038001. 10.1117/1.Jbo.26.3.038001.
48. Schultz, M., Baumhoff, P., Maier, H., Teudt, I.U., Kruger, A., Lenarz, T., and Kral, A. (2012). Nanosecond laser pulse stimulation of the inner ear-a wavelength study. Biomed. Opt. Express *3*, 3332-3345. 10.1364/boe.3.003332.
49. Thompson, A.C., Fallon, J.B., Wise, A.K., Wade, S.A., Shepherd, R.K., and Stoddart, P.R. (2015). Infrared neural stimulation fails to evoke neural activity in the deaf guinea pig cochlea. Hear. Res. *324*, 46-53. 10.1016/j.heares.2015.03.005.
50. Baumhoff, P., Kallweit, N., and Kral, A. (2019). Intracochlear near infrared stimulation: Feasibility of optoacoustic stimulation in vivo. Hear. Res. *371*, 40-52. 10.1016/j.heares.2018.11.003.
51. Richter, C.P., Bayon, R., Izzo, A.D., Otting, M., Suh, E., Goyal, S., Hotaling, J., and Walsh Jr., J.T. (2008). Optical stimulation of auditory neurons: Effects of acute and chronic deafening. Hear. Res. *242*, 42-51. 10.1016/j.heares.2008.01.011.
52. Tan, X., Jahan, I., Xu, Y., Stock, S., Kwan, C.C., Soriano, C., Xiao, X., Garcia-Anoveros, J., Fritzsch, B., and Richter, C.P. (2018). Auditory neural activity in congenitally deaf mice induced by infrared neural stimulation. Sci. Rep. *8*, 388. 10.1038/s41598-017-18814-9.
53. Young, H.K., Tan, X., Xia, N., and Richter, C.P. (2015). Target structures for

cochlear infrared neural stimulation. Neurophotonics *2*, 025002. 10.1117/1.NPh.2.2.025002.

54. Guo, Z.V., Hires, S.A., Li, N., O'Connor, D.H., Komiyama, T., Ophir, E., Huber, D., Bonardi, C., Morandell, K., Gutnisky, D., et al. (2014). Procedures for behavioral experiments in head-fixed mice. PloS one *9*, e88678. 10.1371/journal.pone.0088678.

55. Toda, K., Lusk, N.A., Watson, G.D.R., Kim, N., Lu, D., Li, H.E., Meck, W.H., and Yin, H.H. (2017). Nigrotectal stimulation stops interval timing in mice. Curr. Biol. *27*, 3763-3770.e3763. 10.1016/j.cub.2017.11.003.

56. Kaneko, S., Niki, Y., Yamada, K., Nasukawa, D., Ujihara, Y., and Toda, K. (2022). Systemic injection of nicotinic acetylcholine receptor antagonist mecamylamine affects licking, eyelid size, and locomotor and autonomic activities but not temporal prediction in male mice. Mol. Brain. *15*, 77. 10.1186/s13041-022-00959-y.

57. Yamamoto, K., Yamada, K., Yatagai, S., Ujihara, Y., and Toda, K. (2022). Spatiotemporal Pavlovian head-fixed reversal learning task for mice. Mol. Brain. *15*, 78. 10.1186/s13041-022-00952-5.

58. Abràmoff, M.D., Magalhães, P.J., and Ram, S.J. (2004). Image processing with ImageJ. Biophotonics Int. *11*, 36-42.

59. Schneider, C.A., Rasband, W.S., and Eliceiri, K.W. (2012). NIH Image to ImageJ: 25 years of image analysis. Nat. Methods. *9*, 671-675. 10.1038/nmeth.2089.

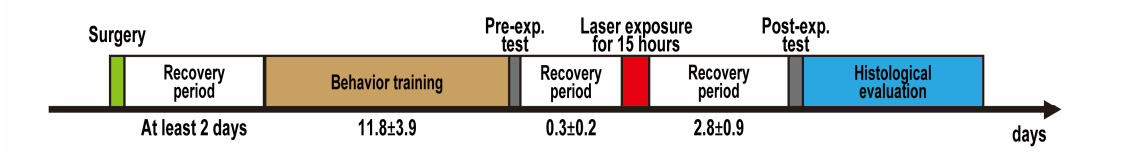

Fig. 1. Time course of the experiment. Before head-fixed classical conditioning, surgery was performed to set the head plate and recording electrode on the subjects and to impair hearing sensitivity in the right ear. At least two days after the surgery, the training session was conducted to associate the relationship between the auditory cue and the liquid reward for 11.8 ± 3.9 days (Mean ± SEM, n=18). The pre-exposure test was conducted after the training was completed. Subsequently, continuous laser exposure was presented for 15 h after recovery (0.3 ± 0.2 days). The cochlear response was recorded during the laser exposure. The post-exposure test was carried out 2.8±0.9 (Mean±SEM) days after the laser exposure. Finally, the subjects were euthanized on the same day as the post-exposure test, and histological inspection was performed.

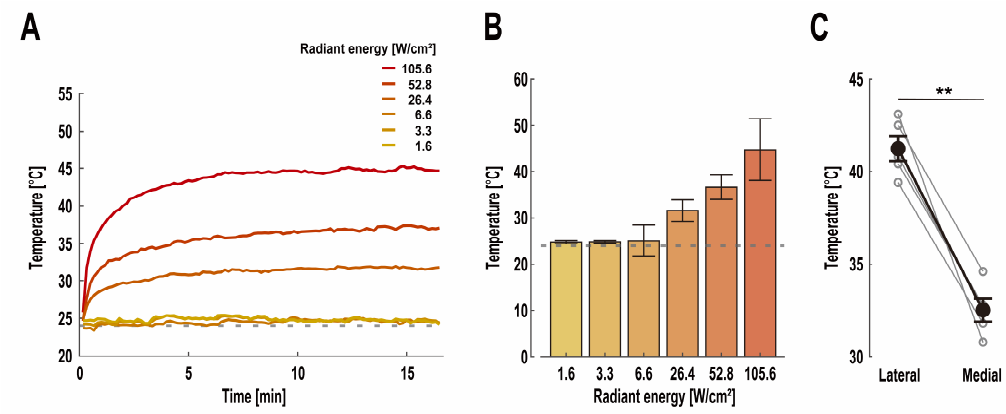

Fig. 2. Thermal elevation of the cochlear surface caused by laser irradiation. (A) Time course of the average temperature rise on the irradiation site of the cochlear surface. (B) Surface temperature at 10 min after the laser onset in (A). Error bars indicate the standard deviation (1.6 W/cm^2: n = 3, others: n = 4). (C) Temperature difference between the lateral and medial sides of the cochlear surface following the laser irradiation of 105.6 W/cm^2 (n=5). Glay open circles show the temperature in each cochlea. In (A) and (B), the gray dotted line shows the room temperature (24 °C). Error bars describe the standard error of the mean. **: $P < 0.01$.

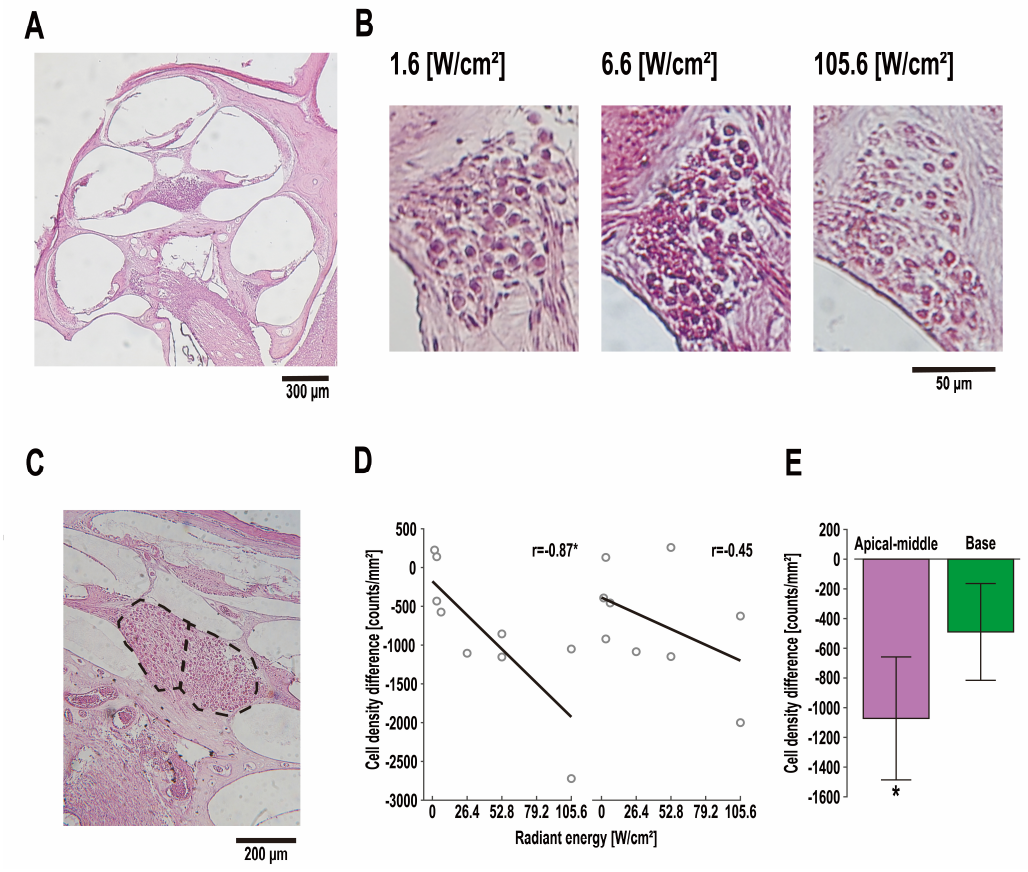

Fig. 3. Laser-induced lesion in spiral ganglion neurons. (A) Horizontal section of laser irradiated cochlea showing all turns (radiant energy: 6.6 W/cm^2). (B) Density of spiral ganglion neurons in the lateral side of the basal turn after laser exposure of 1.6 W/cm^2 (left), 6.6 W/cm^2 (middle), and 105.6 W/cm^2 (right). (C) Lateral (left) and medial (right) sides of the spiral ganglion neuron density in middle turn. The dotted line separates the lateral and medial sides of the spiral ganglion area in the middle turn. (D) Change in the cell density after laser exposure on lateral (left) and medial (right) sides of the cochlea.

757 The cell density difference was defined as the mean spiral ganglion density difference
758 between the laser irradiated (left ear) and the opposite (right ear) cochlea. Gray open
759 circles indicate individual data (n=9). Correlation coefficients were calculated using
760 Pearson's correlation analysis. (E) Mean cell density difference between the laser
761 irradiated and opposite cochlea in apical-middle (left) and basal (right) turn on the lateral
762 side. Data from all radiant energy conditions were pooled in the analysis. *: $P < 0.05$.
763
764

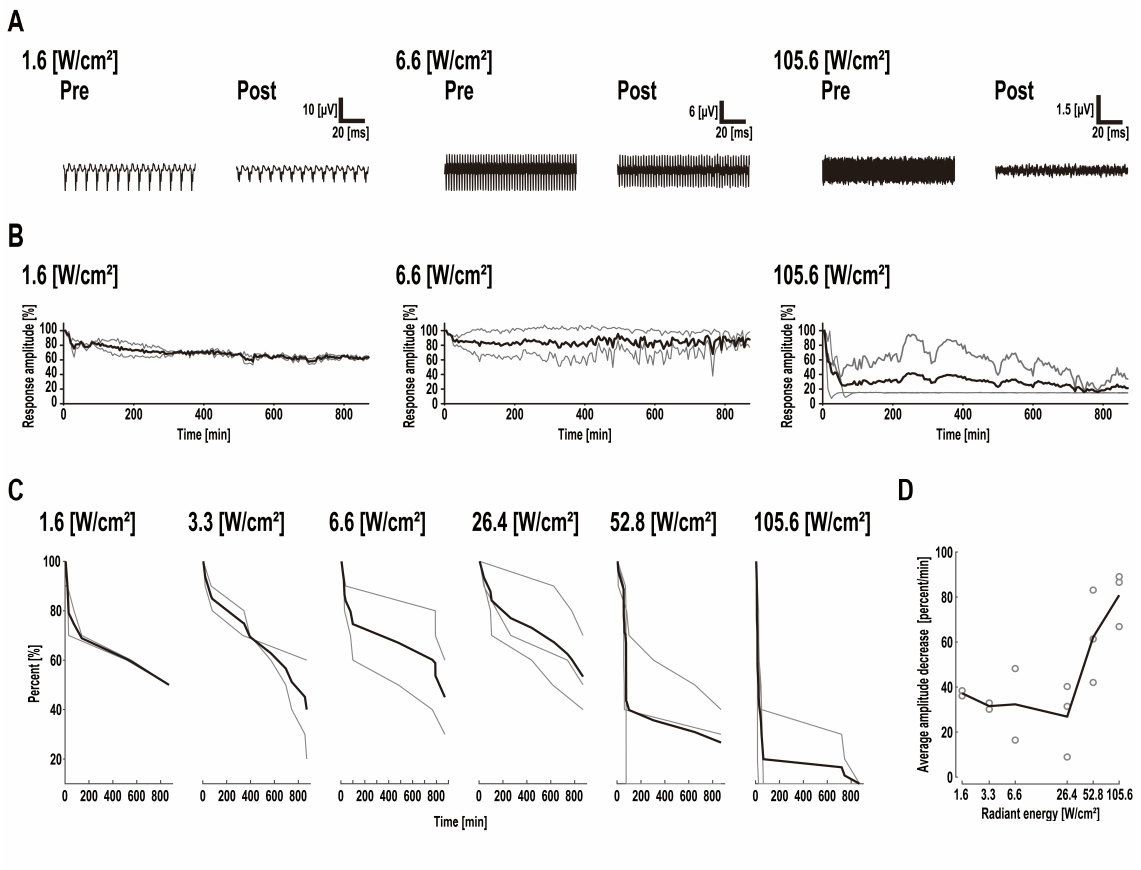

Fig. 4. Cochlear function assessment during continuous laser exposure. (A) Cochlear response during continuous pulsed laser irradiation of 1.6 (left), 6.6 (middle), and 105.6 (right) W/cm^2 (i.e., 125, 500, and 8000 pulses/s). (B) Time course of the cochlear response amplitude elicited by the 1.6 (left), 6.6 (middle), and 105.6 (right) W/cm^2 laser stimulation. (C) Relationship between laser irradiation time and percent of the response amplitude. (D) Average amplitude decrease caused by continuous laser irradiation depending on the radiant energy. Gray open circles indicate individual data (n=15). Gray lines in (B) and (C) show individual data.

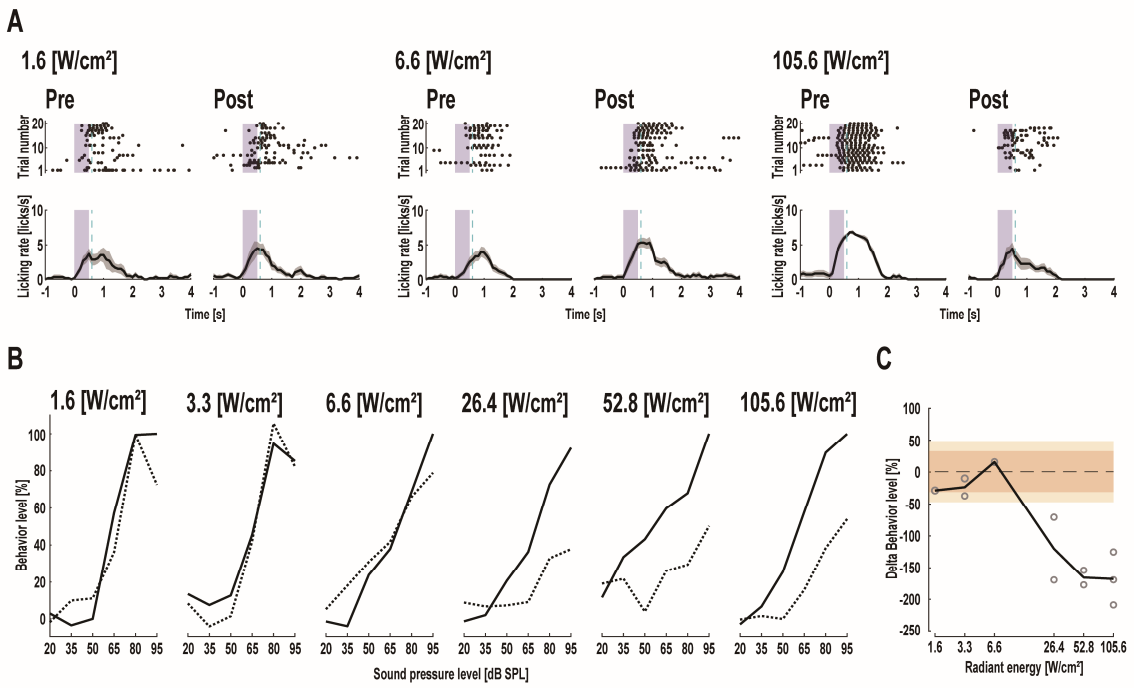

Fig. 5. Influence of continuous laser irradiation on the auditory-evoked behavioral response. (A) Auditory-evoked licking behavior pre- and post-laser exposure of 1.6 (left), 6.6 (middle), and 105.6 (right) W/cm^2. Individual trials and mean peri-stimulus time histograms (PSTH) of the licking behavior elicited by auditory stimuli (80 dB SPL) are shown in top and bottom figures, respectively. The blue zones indicate auditory stimulation periods. The light blue dotted lines show the reward timing in the training trials. Black plots in the top figure show licking timing. (B) Behavioral level alternation after continuous laser irradiation. Solid and dotted lines show pre- and post-behavioral levels, respectively. The behavioral level was determined as the ratio of delta licking rate

785 over the maximum delta licking rate of the pre-laser exposure (1.6 W/cm^2: n=1, 3.3
786 W/cm^2: n=2, 6.6 W/cm^2: n=2, 26.4 W/cm^2: n=2, 52.8 W/cm^2: n=2, 105.6 W/cm^2: n=3).
787 (C) Change in the delta behavioral level between pre- and post-laser exposure. In the
788 control condition, delta behavioral level was measured by comparing the pre- and post-
789 placing the subjects on the experimental setup for 15 h (n=9). Gray dotted line shows the
790 mean of the delta behavioral level in the control condition, and colored areas indicate two
791 (red) and three (orange) standard deviations. The safety margin was determined as the
792 mean ± three standard deviations (i.e., orange area). Gray open cycles represent delta
793 behavioral response in each subject (n = 18).
794
795
796
797

Supplemental Figures

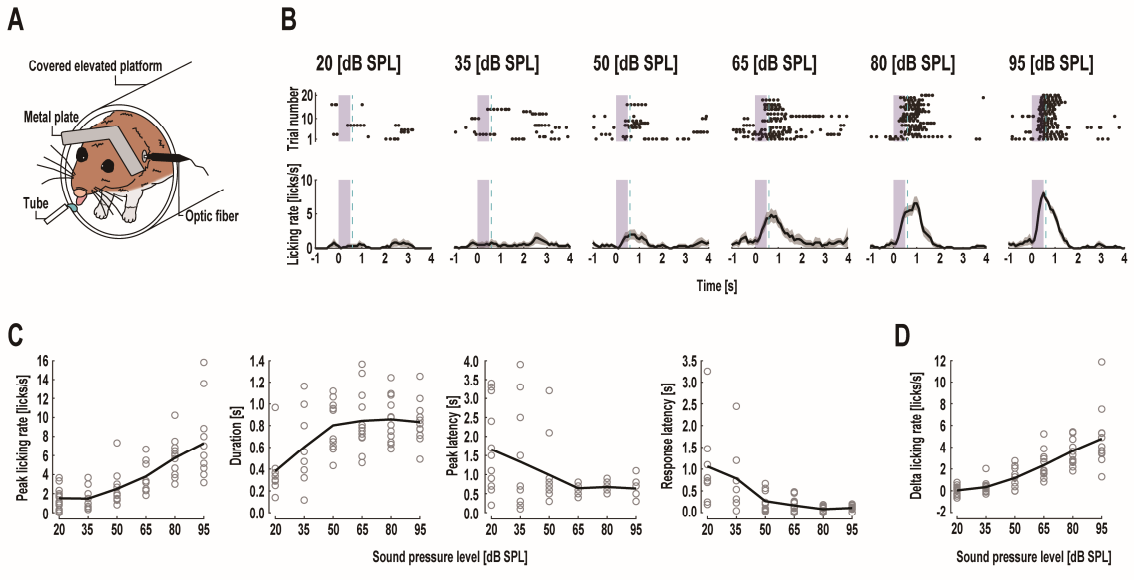

Supplemental Fig. 1. Auditory-induced licking behavior in head-fixed Mongolian gerbils and behavioral profile depending on the sound pressure level. (A) Schematic of the head-fixed setup. We investigated the perception of auditory stimuli by using head-fixed classical conditioning. A drop of water was delivered through the tube after presenting white noise, and the timing of licks was recorded using a touch sensor, as in previous studies. (B) Individual trial (top) and mean peri-stimulus time histogram (PSTH) (bottom) of the licking behavior elicited by auditory stimuli with various sound pressure levels. The blue zones indicate auditory stimulation periods. The light blue dotted lines show the reward timing in the training trials. Black plots in the top figure show licking

timing. Increasing the intensity of white noise elicited a systematic change in behavioral responses. (C) Intensity dependence of the peak licking rate, duration, peak latency, and response latency. As the sound pressure level increased from 20 to 95 dB SPL, peak licking rate was increased from 1.52 to 7.28 licks/s, duration was increased from 0.38 to 0.83 s, peak latency was decreased from 1.66 to 0.63 s, response latency was decreased from 1.06 to 0.11 s. (D) Mean auditory-evoked delta licking rate. The delta licking rate was defined as the response amplitude to quantify the response amplitude of licking behavior. The delta licking rate significantly increased from 0.04 to 4.78 licks/s depending on the intensity of the white noise. In (C) and (D), the open grey cycles show the individual data (n=12).

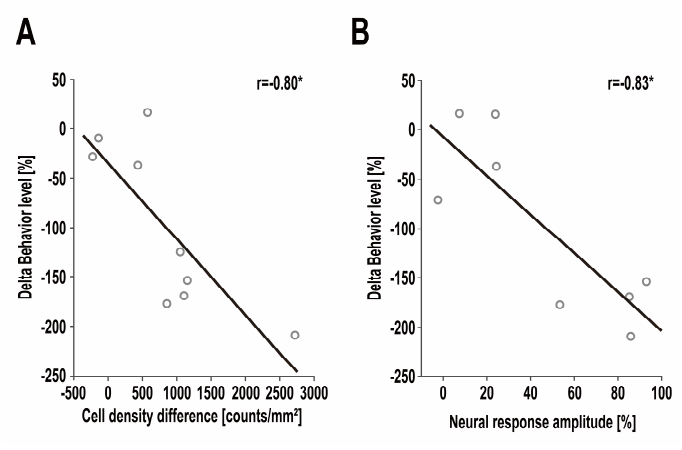

Supplemental Fig. 2. Change in the delta behavioral level depending on the decrease in the cell density difference (A) and neural response amplitude (B). Histological and behavioral data (n=9) or electrophysiological and behavioral data (n=8) were obtained from the subjects. The correlation coefficients were calculated using Pearson's correlation analysis. As the spiral ganglion neuron density decreased, the delta behavioral level significantly decreased (r=-0.80, P<0.05, Pearson's correlation analysis). A similar tendency was observed in the relationship between the decrement of the cochlear response and behavioral response; the decreasing amplitude of the cochlear response significantly reduced the behavioral response (r=-0.83, P<0.05, Pearson's correlation analysis). These results suggest that auditory perception is affected by the physiological deterioration of the cochlea. The open circles indicate individual data. *: $P < 0.05$.